Biochemical and Biophysical Research Communications 441 (2013) 377–382

Contents lists available at ScienceDirect

Biochemical and Biophysical Research Communications

journal homepage: www.elsevier.com/locate/ybbrc

Insights into the carboxyltransferase reaction of pyruvate carboxylase from the structures of bound product and intermediate analogs

Adam D. Lietzan, Martin St. Maurice *

Department of Biological Sciences, Marquette University, Milwaukee, WI 53201, USA

ARTICLE INFO

Article history:
Received 27 September 2013
Available online 22 October 2013

Keywords:
Biotin-dependent carboxylase
Carboxyltransferase
Pyruvate carboxylase

ABSTRACT

Pyruvate carboxylase (PC) is a biotin-dependent enzyme that catalyzes the MgATP- and bicarbonate-dependent carboxylation of pyruvate to oxaloacetate, an important anaplerotic reaction in central metabolism. The carboxyltransferase (CT) domain of PC catalyzes the transfer of a carboxyl group from carboxybiotin to the accepting substrate, pyruvate. It has been hypothesized that the reactive enolpyruvate intermediate is stabilized through a bidentate interaction with the metal ion in the CT domain active site. Whereas bidentate ligands are commonly observed in enzymes catalyzing reactions proceeding through an enolpyruvate intermediate, no bidentate interaction has yet been observed in the CT domain of PC. Here, we report three X-ray crystal structures of the *Rhizobium etli* PC CT domain with the bound inhibitors oxalate, 3-hydroxypyruvate, and 3-bromopyruvate. Oxalate, a stereoelectronic mimic of the enolpyruvate intermediate, does not interact directly with the metal ion. Instead, oxalate is buried in a pocket formed by several positively charged amino acid residues and the metal ion. Furthermore, both 3-hydroxypyruvate and 3-bromopyruvate, analogs of the reaction product oxaloacetate, bind in an identical manner to oxalate suggesting that the substrate maintains its orientation in the active site throughout catalysis. Together, these structures indicate that the substrates, products and intermediates in the PC-catalyzed reaction are not oriented in the active site as previously assumed. The absence of a bidentate interaction with the active site metal appears to be a unique mechanistic feature among the small group of biotin-dependent enzymes that act on α-keto acid substrates.

1. Introduction

Pyruvate carboxylase (PC; EC 6.4.1.1) is a multifunctional, biotin-dependent enzyme that catalyzes the bicarbonate- and MgATP-dependent carboxylation of pyruvate to oxaloacetate, an important anaplerotic reaction in central metabolism (reviewed in [1]). Aberrant enzyme activities and protein expression levels are associated with Type II diabetes, tumor cell proliferation, and bacterial virulence. In all eukaryotes and most prokaryotes, PC is a homotetramer, with each monomer consisting of four functional domains: the biotin carboxylase (BC) domain, the carboxyltransferase (CT) domain, the biotin carboxyl carrier protein (BCCP) domain and the central allosteric domain. The catalytic reaction requires a covalently tethered biotin cofactor, which is initially carboxylated in the BC domain with the cleavage of MgATP. Following carboxylation, carboxybiotin physically translocates to the CT domain where the carboxyl group is transferred to pyruvate to form oxaloacetate.

While the reaction mechanism for the BC domain of PC has been extensively investigated, detailed insights into the CT domain reaction have only recently emerged. For example, the CT domain of *Rhizobium etli* PC (*Re*PC) utilizes a conserved Thr882 to shuttle a proton from pyruvate to the biotin enolate [2], while Arg548, Gln552, and Arg621 serve to stabilize the enolpyruvate intermediate [3,4], and Asp590 and Tyr628 form a substrate-induced biotin binding pocket to accommodate the insertion of carboxybiotin into the active site [5]. Recent X-ray crystal structures of PC have shown pyruvate bound in the active site [5–7] but, surprisingly, pyruvate does not coordinate the active site metal through a bidentate interaction. This unexpected pyruvate binding pose raises questions about the role of the metal ion in the carboxyltransferase reaction. A structure of the product, oxaloacetate, bound in the active site would further clarify the position of reactants relative to the active site metal ion. However, attempts at determining a structure of PC with bound oxaloacetate have not been successful, largely due to

Abbreviations: APS, advanced photon source; BC, biotin carboxylase; BCCP, biotin carboxyl carrier protein; BisTris, 2-[Bis(2-hydroxyethyl)amino]-2-(hydroxymethyl)propane-1,3-diol; CT, carboxyl transferase; LS-CAT, Life Sciences Collaborative Access Team; PC, pyruvate carboxylase; PEG, poly(ethylene glycol); *Re*PC, *Rhizobium etli* pyruvate carboxylase; *Sa*PC, *Staphylococcus aureus* pyruvate carboxylase; TMACl, tetramethylammonium chloride.

* Corresponding author. Address: Department of Biological Sciences, Marquette University, PO Box 1881, Milwaukee, WI 53201, USA. Fax: +1 414 288 7357.
E-mail address: martin.stmaurice@marquette.edu (M. St. Maurice).

0006-291X/$ - see front matter © 2013 Elsevier Inc. All rights reserved.
http://dx.doi.org/10.1016/j.bbrc.2013.10.066

the relatively rapid rate of spontaneous oxaloacetate decarboxylation [5,6].

Here we report three X-ray crystal structures of the CT domain from *Re*PC with bound analogs of the reaction intermediate and product (Fig. 1). The structure with oxalate, a stereoelectronic mimic of the enolpyruvate intermediate, suggests that the metal center does not directly participate in the reaction mechanism. Taken together with the structures of the CT domain with the product analogs, 3-hydroxypyruvate and 3-bromopyruvate, these structures contribute new details to the mechanistic description of the PC catalyzed reaction.

2. Materials and methods

2.1. General

Oxalate and 3-bromopyruvate were purchased from Alfa Aesar. All other materials, including 3-hydroxypyruvate, were purchased from Sigma–Aldrich. ΔBCΔBCCP *Re*PC was previously subcloned into a modified pET-28a vector for recombinant expression in λ(DE3) lysogenized *Escherichia coli* BL21Star [5].

2.2. Protein purification

ΔBCΔBCCP *Re*PC protein was purified and concentrated as previously described [5].

2.3. Isothermal titration calorimetry

ITC experiments were performed using a Microcal ITC200 (GE Life Sciences) with 296 μM ΔBCΔBCCP*Re*PC in 20 mM HEPES buffer (pH 7.5) in the ITC cell. This was titrated with 10 mM pyruvate or 3 mM oxalate in 20 mM HEPES buffer (pH 7.5). The binding isotherm was calculated after subtracting a control titration into an ITC cell containing 20 mM HEPES buffer (pH 7.5). Binding isotherms were fit to a one site binding model.

2.4. Protein crystallization

2.4.1. ΔBCΔBCCP RePC co-crystallization with oxalate

ΔBCΔBCCP *Re*PC was crystallized using the batch crystallization method under oil, as previously described [5]. Crystallization conditions for the three crystal structures were nearly identical. For the ΔBCΔBCCP *Re*PC structure containing oxalate, the protein solution consisting of 10 mg/mL ΔBCΔBCCP *Re*PC and 25 mM oxalate was mixed at a 1:1 ratio with the precipitant solution comprised of 11.3% (w/v) PEG 8000, 99 mM BisTris (pH 6.0), and 346 mM tetramethylammonium chloride (TMACl). A seed stock was generated using the seed bead kit from Hampton Research (Aliso Viejo, CA). Briefly, a single apoprotein ΔBCΔBCCP *Re*PC crystal was pulverized in 500 μL of precipitant solution and 0.5 μL of the seed solution was added to the crystallization drop immediately following mixing. The drop was covered with paraffin oil and diamond shaped crystals formed with 2–3 days. After 5–7 days, the crystals were serially transferred in 5% (v/v) glycerol increments from a synthetic mother liquor solution consisting of 11% (w/v) PEG 8000, 70 mM BisTris (pH 6.0), 275 mM TMACl, 5% (v/v) glycerol, and 25 mM oxalate to a cryoprotectant solution consisting of 11.5% (w/v) PEG 8000, 90 mM BisTris (pH 6.0), 300 mM TMACl, 20% (v/v) glycerol, and 25 mM oxalate and flash cooled in liquid nitrogen.

2.4.2. ΔBCΔBCCP RePC with 3-bromopyruvate or 3-hydroxypyruvate

Ligand soaking was necessary to obtain the structures of ΔBCΔBCCP *Re*PC with 3-bromopyruvate or 3-hydroxypyruvate. The protein solution consisting of 12.2 mg/mL ΔBCΔBCCP *Re*PC, was mixed at a 1:1 ratio with the precipitant solution comprised of 11.3% (w/v) PEG 8000, 99 mM BisTris (pH 6.0), and 346 mM TMACl. The crystallization drop was seeded and covered with paraffin oil as described above. Apocrystals of ΔBCΔBCCP *Re*PC were transferred and soaked in a mother liquor solution containing 10% (w/v) PEG 8000, 80 mM BisTris (pH 6.0), 200 mM TMACl, and 80 mM 3-bromopyruvate for 16 h at room temperature. Similarly, apo crystals of ΔBCΔBCCP *Re*PC with 3-hydroxypyruvate were transferred and soaked in an identical mother liquor solution for 24 h with 130 mM 3-hydroxypyruvate in place of 3-bromopyruvate. Crystals were then serially transferred in 5% (v/v) glycerol increments from the synthetic mother liquor solution to a cryoprotectant solution consisting of 11% (w/v) PEG 8000, 90 mM BisTris (pH 6.0), 200 mM TMACl, 80 mM 3-bromopyruvate or 130 mM 3-hydroxypyruvate, and 20% (v/v) glycerol and flash cooled in liquid nitrogen.

2.5. Data collection, structure determination, and refinement

X-ray diffraction data were collected at the Advanced Photon Source (APS, Argonne, IL), beamline LS-CAT (Life Sciences

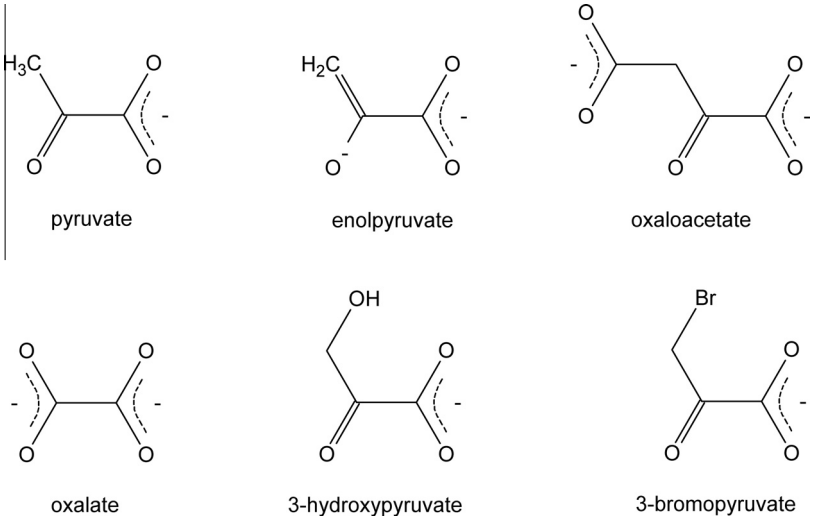

Fig. 1. Structures of the reaction substrate (pyruvate), reaction intermediate (enolpyruvate), reaction product (oxaloacetate), reaction intermediate analog (oxalate), and two reaction product analogs (3-hydroxypyruvate and 3-bromopyruvate).

Collaborative Access Team) 21-ID-G and 21-ID-F on Rayonix MarMosaic 300 CCD and 225 CCD detectors, respectively. The wavelength for all structures was tuned to 0.979 Å and the diffraction images were processed with the HKL2000 suite [8]. The structures were solved by molecular replacement using the structure of ΔBCΔBCCP *Re*PC (pdb i.d. 4JX4) as the search model with the program Phaser [9]. Following molecular replacement, translation/liberation/screw (TLS) refinements were performed using REFMAC [10]. Each monomer was treated as a rigid TLS group. All four monomers in the asymmetric unit were restrained using non-crystallographic symmetry for all models during the entire refinement process. The models were extended by several rounds of manual model building with COOT [11] and successive refinements with REFMAC. Water molecules were added to the models in COOT with subsequent manual verification. Data collection and processing statistics are summarized in Table 1. The atomic coordinates for ΔBCΔBCCP *Re*PC with oxalate, ΔBCΔBCCP *Re*PC with 3-hydroxypyruvate and ΔBCΔBCCP *Re*PC with 3-bromopyruvate have been deposited in the Protein Data Bank as entry 4MFD, 4MFE and 4MIM, respectively.

3. Results and discussion

3.1. Structure of the RePC CT domain with an intermediate analog

The carboxyl transfer reaction in the CT domain of PC is proposed to proceed through a stabilized enolpyruvate intermediate [2]. In the CT active site, carboxybiotin decarboxylates to release CO_2. The resulting biotin enolate abstracts a proton from a nearby conserved threonine (Thr882 in *Re*PC), which, in a concerted step, abstracts a proton from pyruvate to form the enolpyruvate intermediate. The enolpyruvate then attacks the liberated CO_2 to form oxaloacetate [2]. The enolpyruvate is typically depicted as being stabilized through bidentate coordination to the Lewis acid metal at the center of the active site and mutations to residues coordinating this metal ion lead to a complete loss of enzymatic activity in PC [12]. However, to date, none of the crystal structures of PC co-crystallized with pyruvate show the substrate chelating the divalent active site metal through a bidentate interaction [3,6,13,14]. Instead, pyruvate is always oriented with just the carbonyl oxygen oriented toward the metal center and, furthermore, a water molecule is often observed to be bridging this interaction.

Oxalate is the most potent inhibitor reported for PC. It is non-competitive with respect to pyruvate with a reported K_i value of 70 μM [15], 50–130 μM [16], and 12 μM [17] for PC enzymes from yeast, rat liver, and chicken liver, respectively. Oxalate is competitive with respect to oxaloacetate and has a dissociation constant of 8.9 μM for the metal center of chicken liver PC [18]. At neutrality, the two carboxylates of oxalate are deprotonated (pK_{a1} = 1.19; pK_{a2} = 4.22) [19]. In this ionization state, oxalate is a strong chelator of metal ions and shares structural and chemical properties with the enolpyruvate intermediate. Typically, enzymes that catalyze reactions proceeding through an enolpyruvate intermediate, such as pyruvate kinase and phosphoenolpyruvate caboxykinase, are observed to bind oxalate as a bidentate ligand in the crystal structures [20–22].

Table 1
Data collection and refinement statistics.

	ΔBCΔBCCP *Re*PC + oxalate	ΔBCΔBCCP *Re*PC + 3-hydroxypyruvate	ΔBCΔBCCP *Re*PC + 3-bromopyruvate
PDB ID code	4MFD	4MFE	4MIM
Space group	$P2_12_12_1$	$P2_12_12_1$	$P2_12_12_1$
Cell dimensions			
a, *b*, *c* (Å)	86, 157, 245	84, 158, 243	86, 157, 243
α, *β*, *γ* (°)	90, 90, 90	90, 90, 90	90, 90, 90
Resolution range, Å	50.0–2.55 (2.59–2.55)[a]	50.0–2.60 (2.64–2.60)[a]	50.0–2.65 (2.70–2.65)[a]
Redundancy	7.3 (7.1)	5.5 (5.5)	7.1 (6.6)
Completeness (%)	99.8 (99.3)	96.0 (93.2)	99.9 (99.7)
Unique reflections	108 188	91 812	95 052
R_{merge} (%)	8.6 (43.7)	6.6 (43.4)	8.2 (44.3)
Average *I*/*s*	21.1 (4.4)	22.8 (3.3)	24.5 (3.6)
Refinement:			
Resolution range, Å	48.26–2.55 (2.61–2.55)	49.37–2.61 (2.67–2.61)	48.13–2.65 (2.72–2.65)
R_{cryst}	0.193 (0.262)	0.177 (0.238)	0.186 (0.279)
R_{free}	0.240 (0.296)	0.225 (0.298)	0.235 (0.334)
No. protein atoms	17,814	17,488	17,532
No. water molecules	190	169	136
Wilson *B*-value (Å^2)	51.2	59.9	53.8
Average total *B*-factors (B_{TLS} + $B_{residual}$) (Å^2)			
Protein	78.8	78.5	76.9
Chain A	53.2	58.4	56.0
Chain B	69.1	91.2	90.6
Chain C	101.1	74.5	73.4
Chain D	93.5	91.2	88.7
Ligands	62.2	66.6	60.5
Solvent	49.3	56.4	54.9
Ramachandran (%)			
Most favored	90.9	90.4	90.8
Additionally allowed	8.3	8.9	8.7
Generously allowed	0.7	0.7	0.5
Disallowed	0.0	0.0	0.0
r.m.s. deviations			
Bond lengths (Å)	0.0157	0.0156	0.0140
Bond angles (°)	1.638	1.727	1.612

[a] Values in parentheses are for the highest resolution bin.

A truncated construct of *Re*PC was generated that lacked both the BC and BCCP domains and included only the allosteric and CT domains of the enzyme (ΔBCΔBCCP *Re*PC; [5]). Using isothermal titration calorimetry (ITC), the K_D values for pyruvate and oxalate with ΔBCΔBCCP *Re*PC were determined to be ~2 mM and 0.13 mM, respectively. These data indicate that oxalate binds the active site with a 15-fold greater affinity than the *bona fide* substrate, pyruvate. To gain further insights into the catalytic mechanism in the CT domain of PC, this construct was co-crystallized with oxalate in order to probe the binding orientation of an enolpyruvate intermediate analog in the active site of the CT domain.

As previously reported, ΔBCΔBCCP *Re*PC crystallizes in the $P2_12_12_1$ space group and the asymmetric unit is composed of four monomers in a dimer of dimers arrangement [5]. For all structures reported here, all monomers within each asymmetric unit are near identical to one another with the highest r.m.s. deviation for all atoms being 0.3 Å. The CT domain architecture consists of a canonical $\alpha_8\beta_8$ TIM barrel fold with a large C-terminal funnel, comprised of nine α-helices, that leads into the active site at the mouth of the barrel. The active site is centered on the structurally conserved Lewis acid metal, which is either Mn^{2+} or Zn^{2+} [5].

Surprisingly, oxalate does not directly interact with the active site metal ion: the distance between the metal ion and oxalate is 4.5 Å, with a bridging water molecule located 2.3 Å away from the metal (Fig. 2A). Instead, it is positioned in the active site similarly to the substrates pyruvate (green; pdb i.d. 4JX5) and oxamate (yellow; pdb i.d. 4LOC) (Fig. 2B). The planes of the carboxyl moieties for oxalate are staggered such that one carboxyl moiety forms a salt bridge with the guanidinium side-chain of Arg621 and the other maintains hydrogen bond interactions with Arg548 (3.1 Å) and Gln552 (3.3 Å), two residues that are essential for *Re*PC catalysis [4]. Pyruvate and oxamate also interact with Arg621, Arg548 and Gln552, but they adopt a planar conformation in the active site of *Re*PC ([5]; pdb i.d. 4LOC). Because the planes of the oxalate carboxyl moieties are staggered, the carboxyl moiety closest to the metal center is positioned near to Thr882, the residue responsible for transferring a proton to the enolpyruvate intermediate in the oxaloacetate decarboxylation reaction. Additionally, the binding of oxalate appears to be specific, since it promotes a substrate-induced closure of the active site through an interaction between the hydroxyl moiety of Tyr628 and the side chain of Asp590 [5].

The structure of ΔBCΔBCCP *Re*PC with oxalate bound in the active site further clarifies the chemical mechanism in the CT domain of PC. Despite being an excellent metal chelator, oxalate does not form a bidentate interaction with the metal ion located at the center of the active site. This strongly suggests that the enolpyruvate intermediate formed during catalysis is not primarily stabilized through an interaction with the metal center. Instead, the developing negative charge in the enolpyruvate intermediate is stabilized through a salt bridge interaction with the guanidinium of Arg621 and interactions with Arg548, Gln552, and the metal. Mutating Arg548 and Gln552 in *Re*PC results in the complete loss of pyruvate carboxylation activity, further supporting a role for these amino acids in catalysis [4]. Notably, the glutamine/arginine pair

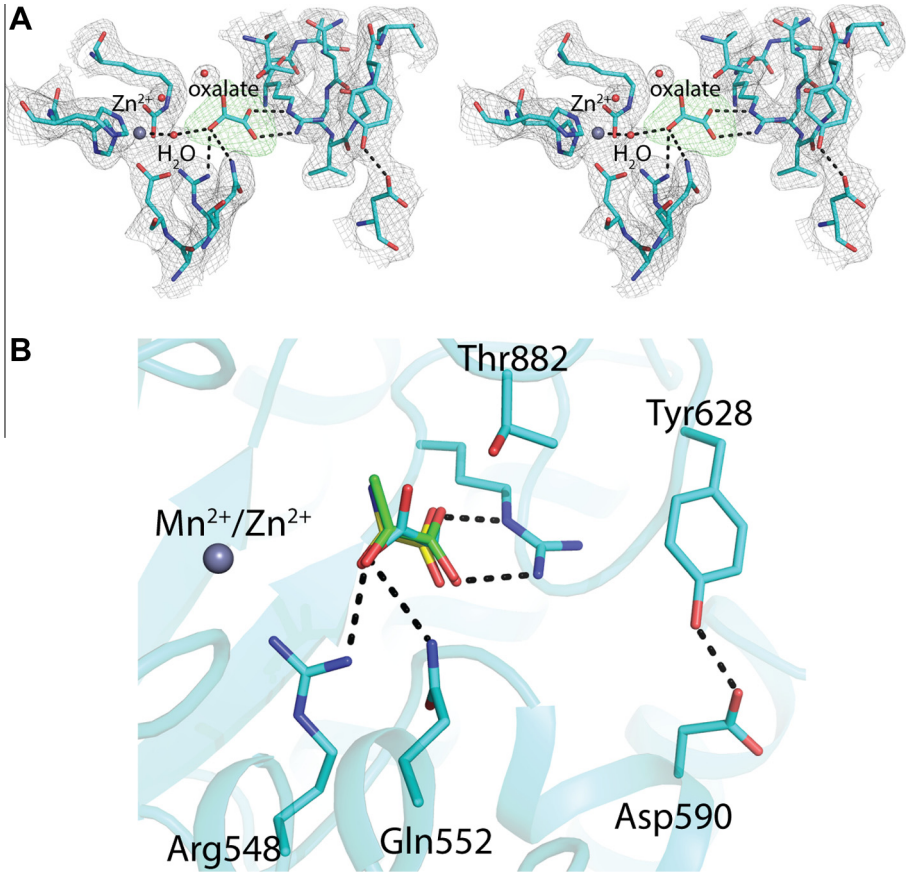

Fig. 2. (A) Stereo view of representative electron density for the active site of ΔBCΔBCCP *Re*PC co-crystallized with oxalate. The $2F_o - F_c$ electron density map is contoured at 1.0 σ and is represented as a grey mesh. The $F_o - F_c$ omit density map is contoured at 3.0 σ and is represented as a green mesh. (B) Structural overlay of ΔBCΔBCCP *Re*PC with oxalate (cyan; monomer A) against the structures of ΔBCΔBCCP *Re*PC with pyruvate (green; pdb i.d. 4JX5 – monomer A) and oxamate (yellow; pdb i.d. 4LOC – monomer A). The rms deviation of the structure with oxalate against the structures with pyruvate and oxamate is 0.17 and 0.20 Å, respectively. (For interpretation of the references to color in this figure legend, the reader is referred to the web version of this article.)

(Arg548/Gln552) is conserved in the broader DRE-TIM metalloenzyme family that catalyzes carbon–carbon bond cleavage on substrates that proceed through stabilization of an enolate intermediate [23] . As opposed to a bidentate interaction with the metal ion, the binding orientation adopted by pyruvate and oxalate permits free rotation about the C1–C2 bond to allow C3 to be properly positioned for proton transfer between C3 and the hydroxyl moiety of Thr882 and to orient the carbanion at C3 to attack the liberated CO_2 from biotin. Interestingly, the only available structures of a homologous enzyme with bound products and substrates are from the 5S subunit of transcarboxylase, which also revealed that the substrates and products do not directly interact with the active site metal ion [24].

3.2. Structures of the CT domain from RePC with product analogs

To date, attempts at capturing structures of oxaloacetate, the reaction product, in the active site of PC have been unsuccessful [6]. Both co-crystallization and soaking attempts with oxaloacetate have resulted in electron density corresponding to pyruvate in the active site [6]. Capturing structures of oxaloacetate in the active site is complicated by the ability of the CT domain to catalyze the decarboxylation of oxaloacetate [5]. In order to gain insights into how oxaloacetate is positioned in the active site of PC, apo crystals of ΔBCΔBCCP *Re*PC were soaked with 3-hydroxypyruvate and 3-bromopyruvate, structural mimics of oxaloacetate and inhibitors of the carboxyl transfer reaction.

3-Hydroxypyruvate, which is a non-competitive inhibitor with respect to MgATP (K_i = 5.5 mM), HCO_3^- (K_i = 7.1 mM), and pyruvate (K_i = 5.4 mM) for the pyruvate carboxylation reaction from *Thiobacillus novellus* PC [25,26], binds in the active site of ΔBCΔBCCP *Re*PC in a similar orientation to pyruvate. Like pyruvate, the carboxyl moiety of 3-hydroxypyruvate forms a salt bridge interaction with the guanidinium moiety of Arg621, while the C2 carbonyl oxygen is within hydrogen bonding distance to the side chains of Arg548 and Gln552 (Fig. 3A). Interestingly, the hydroxyl moiety at C3 of 3-hydroxypyruvate is positioned in close proximity to the side chain of Thr882. The position occupied by the hydroxyl moiety is likely to represent the position at which enolpyruvate is carboxylated during the reaction. Like pyruvate, oxamate, and oxalate [5,6]; pdb i.d. 4LOC), 3-hydroxypyruvate is not a bidentate ligand and the binding of 3-hydroxpyruvate promotes the closed conformation of the active site.

Halogenating the C3 position of pyruvate results in effective, specific inhibitors of PC (reviewed in [27]). For instance, fluoropyruvate is a non-competitive inhibitor with respect to pyruvate (K_i = 0.17 mM) for the pyruvate carboxylation reaction [17], with pulse NMR data suggesting that it prevents pyruvate coordination in the active site [18]. Further, 10 mM fluoropyruvate and chloropyruvate inhibit gluconeogenesis by 85% and >95%, respectively, in the rat liver by modulating PC activity [28]. Given that halogenated derivatives of pyruvate are potent inhibitors of PC, we determined the structure of ΔBCΔBCCP *Re*PC with 3-bromopyruvate.

3-Bromopyruvate binds in the active site of ΔBCΔBCCP *Re*PC in a similar manner to 3-hydroxypyruvate (Fig. 3B). The carboxyl moiety of 3-bromopyruvate forms a salt bridge interaction with the guanidinium moiety of Arg621, and the bromine atom is positioned towards the side-chain of Thr882, much like the C3 hydroxyl moiety of 3-hydroxypyruvate. However, a weaker binding orientation for 3-bromopyruvate, modeled at 0.2 occupancy,

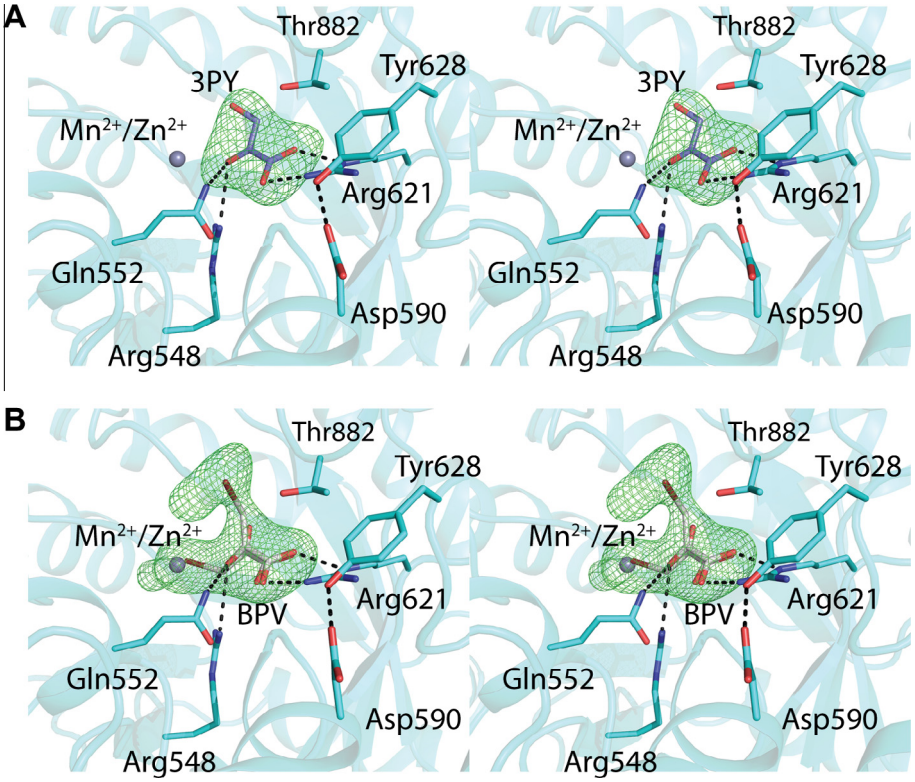

Fig. 3. Representative omit maps for (A) 3-hydroxypyruvate (3PY; purple) and (B) 3-bromopyruvate (BPV; grey) in the active site of ΔBCΔBCCP *Re*PC. The electron density maps are contoured at 3.0 σ. (For interpretation of the references to color in this figure legend, the reader is referred to the web version of this article.)

results in the bromine atom being positioned 2.3 Å away from the active site metal. Normally, the active site metal is octahedrally coordinated by the side chains of Asp549, His747, His749, carbamylated Lys718 and a water molecule. In this second binding mode, 3-bromopyruvate displaces the water molecule and directly interacts with the metal center. This interaction may explain the enhanced potency of halogenated pyruvate derivatives for PC.

3-Bromopyruvate has been described as an anti-cancer agent with a wide range of possible targets required for energy metabolism in tumor cells [29]. Most recently, 3-bromopyruvate has also been described as a novel antifungal agent against human pathogens such as *Cryptococcus neoformans* [30]. While it is recognized that 3-bromopyruvate targets multiple metabolic pathways, to our knowledge PC has not been recognized as a specific target for 3-bromopyruvate. Based on the current findings, PC inhibition should be considered when interpreting the mechanism of cellular inhibition for 3-bromopyruvate and other halogenated derivatives of pyruvate.

Acknowledgments

This work was supported by the National Institute of Health grant GM070455 to W.W. Cleland, John C. Wallace, Paul V. Attwood and Martin St. Maurice. Adam D. Lietzan is supported by a Schmitt fellowship from the Arthur J. Schmitt Foundation. Use of the Advanced Photon Source was supported by U.S. Department of Energy, Office of Science, Office of Basic Energy Sciences, under contract No. DE-AC02-06CH11357. Use of the LS-CAT Sector 21 was supported by the Michigan Economic Development Corporation and the Michigan Technology Tri-Corridor for the support of this research program (Grant 085P1000817). The ITC experiments for ΔBCΔBCCP *Re*PC with oxalate and pyruvate were performed on a microcal iTC200 by Verna Frasca at GE Healthcare Life Sciences.

References

[1] S. Jitrapakdee, M. St. Maurice, I. Rayment, W.W. Cleland, J.C. Wallace, P.V. Attwood, Structure, mechanism and regulation of pyruvate carboxylase, Biochem. J. 413 (2008) 369–387.
[2] T.N. Zeczycki, M. St. Maurice, S. Jitrapakdee, J.C. Wallace, P.V. Attwood, W.W. Cleland, Insight into the carboxyl transferase domain mechanism of pyruvate carboxylase from *Rhizobium etli*, Biochemistry 48 (2009) 4305–4313.
[3] L.P. Yu, S. Xiang, G. Lasso, D. Gil, M. Valle, L. Tong, A symmetrical tetramer for *S. aureus* pyruvate carboxylase in complex with coenzyme A, Structure 17 (2009) 823–832.
[4] S. Duangpan, S. Jitrapakdee, A. Adina-Zada, L. Byrne, T.N. Zeczycki, M. St. Maurice, W.W. Cleland, J.C. Wallace, P.V. Attwood, Probing the catalytic roles of Arg548 and Gln552 in the carboxyl transferase domain of the *Rhizobium etli* pyruvate carboxylase by site-directed mutagenesis, Biochemistry 49 (2010) 3296–3304.
[5] A.D. Lietzan, M. St. Maurice, A substrate-induced biotin binding pocket in the carboxyl transferase domain of pyruvate carboxylase, J. Biol. Chem. 288 (2013) 19915–19925.
[6] S. Xiang, L. Tong, Crystal structures of human and *Staphylococcus aureus* pyruvate carboxylase and molecular insights into the carboxyltransfer reaction, Nat. Struct. Mol. Biol. 15 (2008) 295–302.
[7] L.P. Yu, C.Y. Chou, P.H. Choi, L. Tong, Characterizing the importance of the biotin carboxylase domain dimer for *S. aureus* pyruvate carboxylase catalysis, Biochemistry 52 (2013) 488–496.
[8] Z. Otwinowski, W. Minor, Processing of X-ray diffraction data collected in oscillation mode, Method Enzymol. 276 (1997) 307–326.
[9] A.J. McCoy, R.W. Grosse-Kunstleve, P.D. Adams, M.D. Winn, L.C. Storoni, R.J. Read, Phaser crystallographic software, J. Appl. Crystallogr. 40 (2007) 658–674.
[10] M.D. Winn, G.N. Murshudov, M.Z. Papiz, Macromolecular TLS refinement in REFMAC at moderate resolutions, Methods Enzymol. 374 (2003) 300–321.
[11] P. Emsley, K. Cowtan, Coot: model-building tools for molecular graphics, Acta Crystallogr. D Biol. Crystallogr. 60 (2004) 2126–2132.
[12] J. Yong-Biao, M.N. Islam, S. Sueda, H. Kondo, Identification of the catalytic residues involved in the carboxyl transfer of pyruvate carboxylase, Biochemistry 43 (2004) 5912–5920.
[13] M. St. Maurice, L. Reinhardt, K.H. Surinya, P.V. Attwood, J.C. Wallace, W.W. Cleland, I. Rayment, Domain architecture of pyruvate carboxylase, a biotin-dependent multifunctional enzyme, Science 317 (2007) 1076–1079.
[14] A.D. Lietzan, A.L. Menefee, T.N. Zeczycki, S. Kumar, P.V. Attwood, J.C. Wallace, W.W. Cleland, M. St. Maurice, Interaction between the biotin carboxyl carrier domain and the biotin carboxylase domain in pyruvate carboxylase from *Rhizobium etli*, Biochemistry 50 (2011) 9708–9723.
[15] M. Ruiz-Amil, G. De Torrontegui, E. Palacian, L. Catalina, M. Losada, Properties and function of yeast pyruvate carboxylase, J. Biol. Chem. 240 (1965) 3485–3492.
[16] W.R. McClure, H.A. Lardy, M. Wagner, W.W. Cleland, Rat liver pyruvate carboxylase. II. Kinetic studies of the forward reaction, J. Biol. Chem. 246 (1971) 3579–3583.
[17] M.C. Scrutton, M.R. Olmsted, M.F. Utter, Pyruvate carboxylase from chicken liver, Methods Enzymol. 13 (1969) 235–249.
[18] A.S. Mildvan, M.C. Scrutton, M.F. Utter, Pyruvate carboxylase. VII. A possible role for tightly bound manganese, J. Biol. Chem. 241 (1966) 3488–3498.
[19] W. Riemenschneider, M. Tanifuji, Oxalic acid, in: Ullmann's Encyclopedia of Industrial Chemistry, Wiley-VCH Verlag GmbH & Co. KGaA, 2000.
[20] T.M. Larsen, M.M. Benning, I. Rayment, G.H. Reed, Structure of the bis(Mg^{2+})-ATP-oxalate complex of the rabbit muscle pyruvate kinase at 2.1 Å resolution: ATP binding over a barrel, Biochemistry 37 (1998) 6247–6255.
[21] L.W. Tari, A. Matte, U. Pugazhenthi, H. Goldie, L.T. Delbaere, Snapshot of an enzyme reaction intermediate in the structure of the ATP-Mg^{2+}-oxalate ternary complex of *Escherichia coli* PEP carboxykinase, Nat. Struct. Biol. 3 (1996) 355–363.
[22] J.J. Cotelesage, L. Prasad, J.G. Zeikus, M. Laivenieks, L.T. Delbaere, Crystal structure of *Anaerobiospirillum succiniciproducens* PEP carboxykinase reveals an important active site loop, Int. J. Biochem. Cell Biol. 37 (2005) 1829–1837.
[23] F. Forouhar, M. Hussain, R. Farid, J. Benach, M. Abashidze, W.C. Edstrom, S.M. Vorobiev, R. Xiao, T.B. Acton, Z. Fu, J.J. Kim, H.M. Miziorko, G.T. Montelione, J.F. Hunt, Crystal structures of two bacterial 3-hydroxy-3-methylglutaryl-CoA lyases suggest a common catalytic mechanism among a family of TIM barrel metalloenzymes cleaving carbon–carbon bonds, J. Biol. Chem. 281 (2006) 7533–7545.
[24] P.R. Hall, R. Zheng, L. Antony, M. Pusztai-Carey, P.R. Carey, V.C. Yee, Transcarboxylase 5S structures: assembly and catalytic mechanism of a multienzyme complex subunit, EMBO J. 23 (2004) 3621–3631.
[25] A.M. Charles, D.W. Willer, Pyruvate carboxylase from *Thiobacillus novellus*: properties and possible function, Can. J. Microbiol. 30 (1984) 532–539.
[26] A.M. Charles, D.W. Willer, J.M. Scharer, Possible regulation of pyruvate carboxylase from *Thiobacillus novellus* by hydroxypyruvate, Curr. Microbiol. 10 (1984) 265–268.
[27] T.N. Zeczycki, M. St. Maurice, P.V. Attwood, Inhibitors of pyruvate carboxylase, Open Enzym. Inhib. J. 3 (2010) 8–26.
[28] D. Doedens, J. Ashmore, Inhibition of pyruvate carboxylase by chloropyruvic acid and related compounds, Biochem. Pharmacol. 21 (1972) 1745–1751.
[29] M.C. Shoshan, 3-Bromopyruvate: targets and outcomes, J. Bioenerg. Biomembr. 44 (2012) 7–15.
[30] M. Dylag, P. Lis, K. Niedzwiecka, Y.H. Ko, P.L. Pedersen, A. Goffeau, S. Ulaszewski, 3-Bromopyruvate: a novel antifungal agent against the human pathogen *Cryptococcus neoformans*, Biochem. Biophys. Res. Commun. 434 (2013) 322–327.